This is a repository copy of *Tribological performance of an H-DLC coating prepared by PECVD*.

White Rose Research Online URL for this paper:
http://eprints.whiterose.ac.uk/100983/

Version: Accepted Version

Tribological performance of an H-DLC coating prepared by PECVD

J. Solis[a,b*], H. Zhao[a], C. Wang[a], J.A. Verduzco[c], A. S. Bueno[a,d], A. Neville[a]

[a]IFS, University of Leeds, School of Mechanical Engineering, Leeds LS2 9JT, United Kingdom
[b]SEP/SES/TecNM/ IT de Tlalnepantla, DEPI-Mechanical Engineering, 54070,Edo. Méx., Mexico
[c]Instituto de Investigación en Metalurgia y Materiales, UMSNH, P.O. Box 888, 58000, Morelia, Mich., Mexico.
[d]Mechanical Engineering Department, Universidade Federal de São João Del Rei, 170 Praça Frei Orlando, 36307-352 São João Del Rei, Brazil.

*Corresponding author: jsolis@ittla.edu.mx

Abstract

Carbon-based coatings are of wide interest due to their application in machine elements subjected to continuous contact where fluid lubricant films are not permitted. This paper describes the tribological performance under dry conditions of duplex layered H-DLC coating sequentially deposited by microwave excited plasma enhanced chemical vapour deposition on AISI 52100 steel. The architecture of the coating comprised Cr, WC, and DLC (a-C:H) with a total thickness of 2.8 μm and compressive residual stress very close to 1 GPa. Surface hardness was approximately 22 GPa and its reduced elastic modulus around 180 GPa. Scratch tests indicated a well adhered coating achieving a critical load of 80 N. The effect of normal load on the friction and wear behaviours were investigated with steel pins sliding against the actual coating under dry conditions at room temperature (20± 2 °C) and 35 − 50% RH. The results show that coefficient of friction of the coating decreased from 0.21 to 0.13 values with the increase in the applied loads (10 - 50 N). Specific wear rates of the surface coating also decrease with the increase in the same range of applied loads. Maximum and minimum values were 14×10^{-8} and 5.5×10^{-8} mm^{-3}/N m, respectively. Through Raman spectroscopy and electron microscopy it was confirmed the carbon-carbon contact, due to the tribolayer formation on the wear scars of the coating and pin. In order to further corroborate the experimental observations regarding the graphitisation behaviour, the existing mathematical relationships to determine the graphitisation temperature of the coating/steel contact as well as the flash temperature were used.

Keywords: Hydrogenated Diamond-like carbon; friction; wear; AISI 52100 steel, dry sliding.

1. Introduction.

The quality and functional characteristics of many engineering applications is determined by superimposed mechanical loads and particular requirements on their surface, such as wear resistance or low levels of coefficient of friction (CoF). The use of thin films as the non-stoichiometric hydrogenated amorphous carbon (a-C:H), also named hydrogenated diamond-like carbon (H-DLC), has become widespread for the improvement of performance/life of steel components [1, 2], in which specific properties at particular locations are needed without compromising the bulk material strengths. Furthermore, these coatings are also being used as solid lubricants in the industrial field to improve tribological behaviours of machine components under very clean atmospheres or where fluid lubricants are not permitted. The progressive acceptance of these coatings for the above purposes is due to the mechanical, chemical, electrical and optical properties they exhibit [3, 4]. The deposition of DLCs is commonly obtained by plasma decomposition of a hydrocarbon-rich atmosphere at low substrate temperatures and high deposition rates. The latter is a major advantage for most steels because the annealing temperature is not reached (<200 °C), therefore substrate hardness is not affected.

In spite of the outstanding properties of DLC coatings, the CoF and wear mechanisms depend significantly on the deposition method/parameters [1, 5], variation in environment, either in vacuum or room atmosphere [6], relative humidity [7], the substrate and counterbody materials, the various coating architectures such as multiple or gradient layers, and very importantly, the wearing conditions, i.e. under dry, water, oil or a combination of these [8, 9]. In the case of unlubricated conditions, the influence of loading and sliding velocity on the CoF and wear rates becomes essential. Sharma, et al. [10] put forward variations in the CoF and wear for different loads on the Steel/DLC pair, under ambient and dry conditions,.. The CoF decrease with the increase of normal load for short sliding distances, and for long sliding distances, the CoF decrease with the decrease of normal load. Upon the steady state there seems to be a convergence in the CoF values ranging from 0.05 to 0.2. Meanwhile, wear rates increased with the increase of load. Similar trends were also identified in similar, previous research [11-13]. In contrast, Mo [14] reported very little influence of the normal load on the CoF of a WC/C coating tested under reciprocating sliding against pure titanium. The CoF values found were 0.13 upon the steady state. Therefore, the correlations between tribological performances of a particular DLC and operational conditions have a considerable importance for any possible application for certain machine components. Nevertheless, research has mainly focused on the modification of the physical properties of the new DLC coatings [15, 16] and their evaluations from the tribological and environmental points of view [17]. On the whole, the studies on friction and wear of WC/H-DLC´s for different applied contact pressures and under dry conditions are scarce.

From the number of techniques to deposit hard DLC films, plasma enhanced chemical vapour deposition process (PECVD) is extensively utilised due to the nature of the hydrocarbon gas used as the coatings incorporate more sp^2 and H bonds which make the films softer than the majority of tetrahedral ta-C counterparts? [2, 18]. Furthermore, reactive magnetron sputtering is a relatively new technology that combines magnetron sputtering and PECVD to increase hardness and provide better wear resistance and low friction values in the coated steels [19, 20].

In order to elude the detrimental environment effect of the mating surfaces and to carry off the heat generated through friction, lubrication processes have been successfully used and are designed to influence the friction and wear behaviour of surfaces in contact. However, it is well known that hydrogenated DLC coatings do not react with various lubricants, mainly oil and additives, because of their low surface energy and the lack of attracting polar groups from such oils and additives [21]. In this regard, much research has focused on the synergistic action between carbon-based coatings and new environment-friendly lubricants (lower S and P contents), in the boundary lubrication regime, but it is apparent that the tribological behaviours of DLCs under lubricated conditions are still indistinct [22, 23]. Therefore, since the reactivity of the oil varies with friction surface, the combination of a tribo-coating operating under a lubricated condition is still an aspect under investigation. Thus, while the coefficient of friction has been found higher for the combination of steel/steel compared to the a-C:H/steel combination, there are some cases where the former combination is lower than the latter[24]. It is clear that with the introduction of DLC coatings in existing engineering systems, the main objective for their effective application is to ensure a consistent performance under dry and oil-lubricated conditions. In this context, some of the important studies have been carried out with quite controversial outcomes and/or are not practical for industrial applications because the election of normal loads and sliding velocities are away from real engineering conditions. Evidently, some of these discrepancies may result from different and varying DLCs under investigation. In light of the aforementioned, in this study, a hydrogenated DLC coating has been investigated for its film forming, friction and wear performance in dry sliding under different normal loads. As far as the authors know, there is no study on tribological characteristics of an H-DLC coating with the same composition of layers that resembles the present H-DLC coating architecture. Understanding of the tribological behaviour of this particular coating with the appropriate working conditions will enable expansion in mechanical components coated with functional coatings.

2. Materials and experimental procedures

2.1 Materials and deposition

A WC/a-c:H coating was deposited on AISI 52100 steel plates of dimensions 7 x 7 x 3 mm^3 using an industrial scale Microwave excited Plasma Enhanced Chemical Vapour Deposition (MW-PECVD) Flexicoat 850 system (Hauzer Techno Coating, the Netherlands) in the Advanced Coatings Design Laboratory at the School of Mechanical Engineering of the University of Leeds. The continuous deposition procedure includes deposition of an adherent Cr interlayer (by DC magnetron sputtering) followed by an intermediate hard tungsten carbide (WC) layer (by DC magnetron sputtering and gradual introduction of acetylene gas to chamber). The surface topography of H-DLC coating surface is shown in Fig. 1. This industrial scale PVD/CVD system incorporates two 1000 W microwave plasma sources (2.45 GHz). The negative bias voltage used was 420 V. The substrate was maintained at less than 200 °C. During deposition, control of the substrates temperature is very important for heat sensitive metallic materials such as the steel used in this study. The substrates were cleaned by Ar+ plasma using pulsed DC bias prior to deposition of the adhesion layer. The thickness of the coating was determined by means of the abrasion ball cratering technique utilizing a Calotester apparatus (tribotechnic, France). The total thickness of the a-C:H layer was 2.8 ± 0.2 μm. The compressive residual stress of 0.9 ± 0.05 GPa was determined through substrate deflection before and after H-DLC film deposition on a pure Si wafer. Similar values for this type of coatings were put forward in [25, 26]. The stresses were calculated by using the Stoney equation [27] :

$$\sigma = \frac{4}{3}\left[\frac{E_s t_s}{T L^2 (1-\upsilon)}\right](h - h_0) \quad (GPa) \tag{1}$$

Where E_s is the substrate Elastic Modulus =169 GPa [28], ν is the Poisson´s ratio (0.28) [28], t_s is substrate thickness (0.4 mm), T is the DLC total coating thickness, h - h_o are the maximum deflections of the substrate, before and after the film deposition (a value of 16 μm was measured using white light interferometry), and L is the length (16.7 mm). The thickness ratio $h/t_s \approx 5\%$.
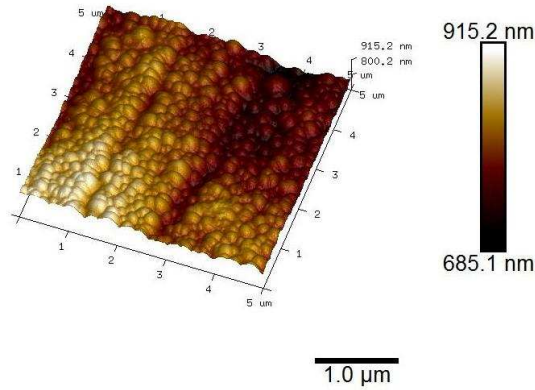
Figure 1. AFM image of the bare H-DLC coating.

2.2 Coating characterisation

A surface roughness of 18 ± 5 nm for this film was evaluated using two-dimensional contacting profilometry (Talysurf5, Taylor-Hobson, UK). Surface roughness data of 8mm trace was analysed to the least square line, with Gaussian filter, 0.25 mm upper cut-off and bandwidth $100 \div 1$. The hardness and the reduced elastic modulus were evaluated by depth-sensing Nano-indentation using a Nano Test (MicroMaterials, Ltd. Wrexham, U.K.), an enclosed box platform with regulated temperature, software suite and micro capture camera. The diamond indenter was a Berkovich tip. The load was incremental with depth from 1 to 50 mN and a matrix of 50 indents was used. The adhesive strength of the coating was tested using a commercial apparatus (millennium 200, TRIBOtechinque, France) fitted with a Rockwell spherical diamond indenter (tip radius of 500 µm). Scratch-tests were performed using progressive loads from 0.1 to 80 N with a load rate of 100 N/min and for a transverse scratch length of 8 mm in dry condition. The scratch tester is equipped with an acoustic emission monitoring sensor. The local chemical bonding structure present at the coated surface, as well as in the wear tracks, was determined using Raman spectroscopy (Renisaw Invia Raman microscope system), and a wave length of the incident laser beam of $\lambda = 488$ nm. All measurements were carried out in air at room temperature (20 ±2 °C) and 35-50% RH.

2.3 Tribological tests

Sliding friction and wear tests of the H-DLC under dry and lubricated conditions were carried out on a pin-on-plate tribometer (Cameron Plint TE77 reciprocating friction rig) in linear/bidirectional motion (Fig. 2). This is a bespoke platform for tribological studies under diverse load and heating conditions. The horizontal friction force is measured by the load cell which is a piezo-electric transducer that

converts the analogue signal into a digital one which is then processed by Labview software. A stainless steel bath is heated by four electrical resistance elements connected to a block positioned below this bath, the heating is then controlled by a thermo-couple that regulates the temperature according to a user defined magnitude. The tribological experiments were carried out using a loaded pin and reciprocated against a stationary H-DLC coated steel in air at ambient temperature.
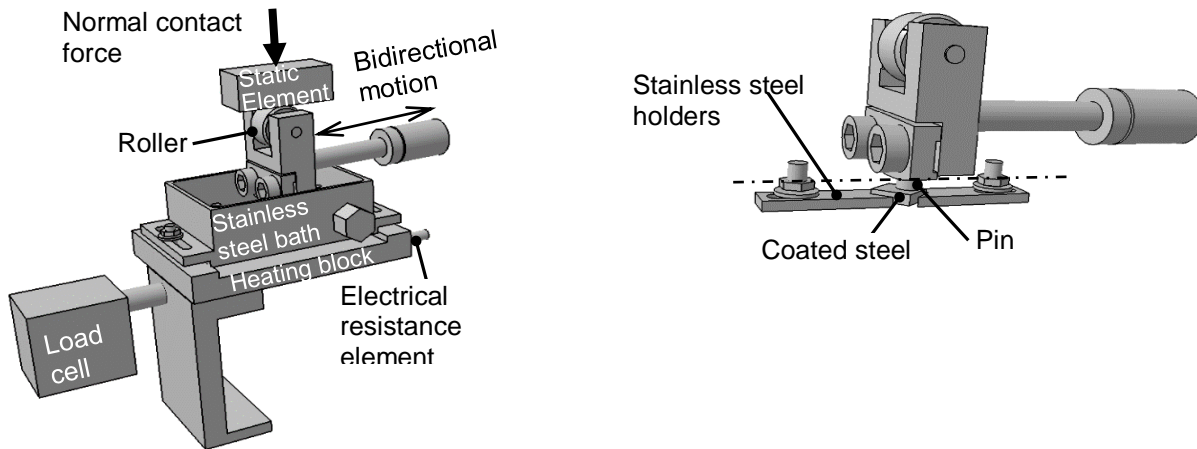

Figure 2. Overview of the reciprocating pin-on-plate set up.

Prior to experimental set up, all holders (both for the sample and for the pin) were sonically cleaned in acetone for 20 min. This procedure was also utilized for the cleaning of samples and pins. Pins were AISI 52100 steel of 20 mm in length, diameter of 6 mm with semi spherical ends of 110-120 mm in radius. The stroke length was set up to 5mm. Material properties are detailed in Table 1. Friction force data was collected every 5 min (1000 data points) for 6 h. To evaluate friction, tests were repeated at least three times for a particular load.

Table 1.   Material properties of the tribopair.

Parameter	Steel (plate and pin)	Coating/Interlayers	
Specification	AISI 52100	H-DLC	
Hardness	~ 11 GPa	20^{+3}_{-0} GPa	
Reduced Elastic modulus	~ 180 GPa	180 ± 10 GPa	
Plate roughness (Ra)	18 ± 5 nm	18 ± 5 nm	
Pin roughness (Ra)	28 ± 2 nm		
Composition (% wt)/coating thickness (μm)	C 0.98–1.10, Cr 1.30–1.60, Mn 0.25–0.45, Si 0.15–0.30, S 0.025, and P 0.025.	~ 0.7	Cr
		~ 0.7	WC
		1.4-1.6	H-DLC
Atomic % of hydrogen		~ 20	

To predict tribological behaviours of H-DLC coatings that will be applied to machine components, the correlations between tribological characteristics of particular H-DLCs coatings and working conditions are of paramount importance. Accordingly, the pin-on-plate configuration, pin semi spherical ends, and the range of normal loads used were intended to emulate the sliding conditions of a piston ring contact of internal combustion engine [29]. The initial Hertzian contact pressure used in this study and the experimental running conditions are shown in Table 2.

Table 2.   Experiment conditions.

Experimental conditions	Magnitude
Load (N)	10, 20, 30, 40 and 50
Maximum Hertzian pressure (MPa)	110, 140, 160, 170 and 190
Frequency (Hz)	10
Average velocity (m s^{-1})	0.1
Temperature (°C)	20 ± 2 (dry condition)
Relative Humidity (%)	35-50
Duration (h)	6

2.4 Surface analysis

2.4.1 Wear measurement

At the start of each test, the plate and pin were sonically cleaned using acetone to degrease and remove any impurities from the surface. Then, they were weighed using a Mettler Toledo AT21 micro-balance with an accuracy of 1 μg. Both samples and pins were again weighed to determine the volume loss. The specific wear rates for the worn parts of the tribocouple were calculated using the Archard relationship:

$$V_L = K\,S\,W \hspace{6cm} (2)$$

where K is the 'Archard coefficient' which is used as an index of wear severity ($mm^3\,N^{-1}\,m^{-1}$), W is the normal load (N), S the sliding distance (m), V_L the loss volume (m^3).

Post wear analysis was also carried out using white light interferometry on a Bruker NP FLEX instrument. Measurements were taken on vertical scanning interferometry mode, scan speed of 1 and 2.5X magnification.

2.4.2 Optical microscope, Scanning Electron Microscope (SEM), Atomic Force Microscope (AFM) and Raman spectroscopy

A Leica optical microscope DM6000 was employed in this study to analyse the worn regions for both tribo systems, i.e. Steel/Steel and H-DLC/Steel. The microstructure, morphology and thickness of the films as well as the worn surfaces were studied using a Zeiss EVO MA15 Variable Pressure and field emission SEM in direct mode. An integrated Oxford Instruments Energy Dispersive X-ray (EDX) analysis system was used to qualitatively and quantitatively evaluate the presence of C and Cr/W outside/inside the wear scar and also to determine the occurrence of material transfer. In depth chemical profiles were obtained by glow discharge optical emission spectroscopy (GDOES). It should be noted that the quantitative EDS and GDOES analysis had the limitation of light elements (Z < 11) and could not be routinely analysed. Thus, hydrogen (Z = 1) did not have characteristic X-rays and therefore it is not shown both in the corresponding EDX analysis and the composition profiles. Surface topography, in turn, was observed with AFM (Bruker, ICON dimension with scan asyst) for the H-DLC and steel surfaces outside and inside the wear scar. AFM scan images were obtained using a silicon tip (cantilever stiffness ~0.4 N/m and tip radius of ~10 nm) in contact mode and a scan area of 5 μm x 5 μm. The carbon coating structure with respect to sp^2/sp^3 ratio was studied by Raman Spectroscopy. A 488nm excitation wave length laser source with 2mW power was used. The extended and static modes were used to detect chemical compound formation and the carbon peaks (disorder D and amorphous graphitic G peaks) both for the coating structure before and after sliding. The scan

range from 800 to 1800 cm^{-1} was applied to identify the carbon peaks. Data was fitted with a Gaussian line shape in order to show the G and D peaks positions and the ratio of peak intensities. The ratio I_D/I_G was considered as an indicator of the carbon sp^2/sp^3 structure and also transfer layer structures. Curve fitting was done considering Full-Width at Half-Maximum (FWHM) as constraint.

3. Results and discussion

3.1 Coating characterisation

The chemical composition in depth showing complete information of the relative interlayers as well as their thickness is shown in Fig. 3. The cross section of the sample (Fig. 3a) shows the duplex layer compound. The surface layer is composed by carbon and hydrogen (the latter not shown) because of the hydrocarbon precursor acetylene, used to deposit the a-c:H. In Fig. 3b, there is an increase in the intensity on the interlayer region (1.37-2.62 μm) with Cr and WC signals. This interlayer WC and H forms a non-stoichiometric hydrogenated tungsten carbide WC:H and as a result, the system is represented as WC/H- a-C:H or WC/H-DLC.
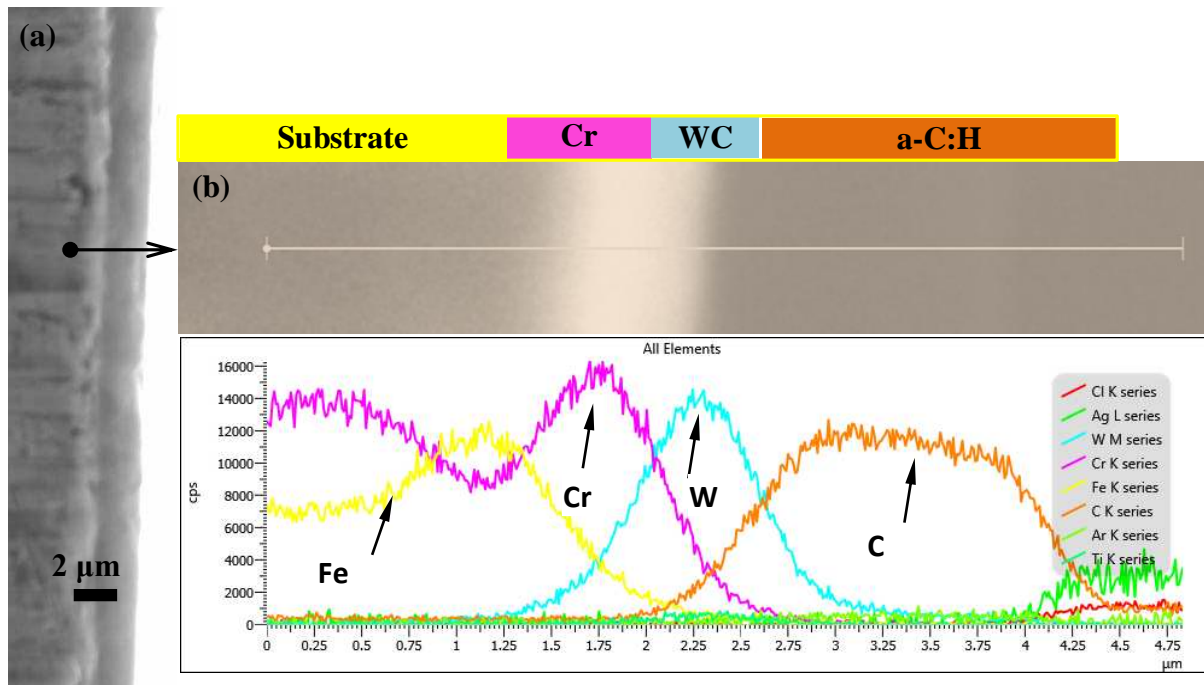

Figure 3. (a) SEM micrograph in cross section and (b) the composition profile of the DLC coating deposited on AISI 53100 steel. The elements Cl and Ag are contaminants due to the manipulation of the sample for the analysis.

9

In order for a coating to be used in one or a number of industrial applications, its adhesive strength is a paramount requirement. Thus, the adhesion of the coating to the substrate is widely measured by means of the scratch test, which provides information regarding the level of adherence in terms of the occurrence of interfacial fractures. Scratch tests indicated that the H-DLC coating was well adhered to the AISI 52100 steel substrate with very little cracking and no evidence of adhesive failure and therefore, no critical failure as shown in Fig. 4. The arrow A points out an early onset of periodic low amplitude acoustic emission (AE) peaks indicating no partial adhesive failure but only microscopic angular cracks at the edge of the groove (64 N). The high amplitude AE peaks pointed out by arrow B corresponds to the total penetration depth (8 mm). There is evidence of transverse semi-circular cracks caused by the higher load (75 N) at the rear of the contact end. It can then be considered a critical load > 80 N for the present coating, which is a more than acceptable value for industrial applications [30] . Despite of the coatings' high hardness, it is clear that there is a plastic deformation along the groove and because there is no evidence of any spallation event or adhesive failure, it can be suggested that the chromium deposited as the adhesion layer between the DLC layer and the substrate, allowed for the relaxation, to a certain extent, of the compressive residual stresses while the ductility to resist the interfacial fracture improves.
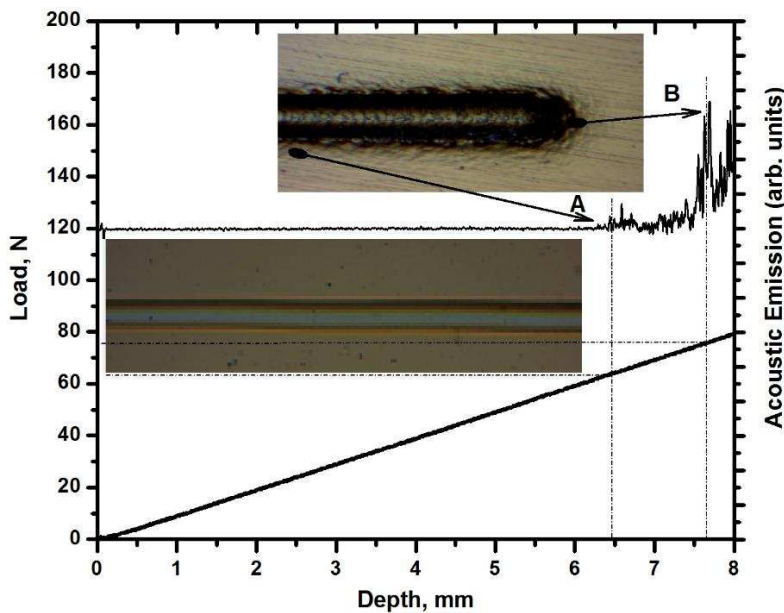

Figure 4. Scratch induced acoustic emission test on the H-DLC deposited by MW-PECVD.

The measured hardness and the reduced elastic modulus from the Nano indentation test on H-DLC coated samples are shown in Fig. 5. Each curve are the averaged result of fifty indents, and the error bars were determined from the standard deviation of those fifty indents.
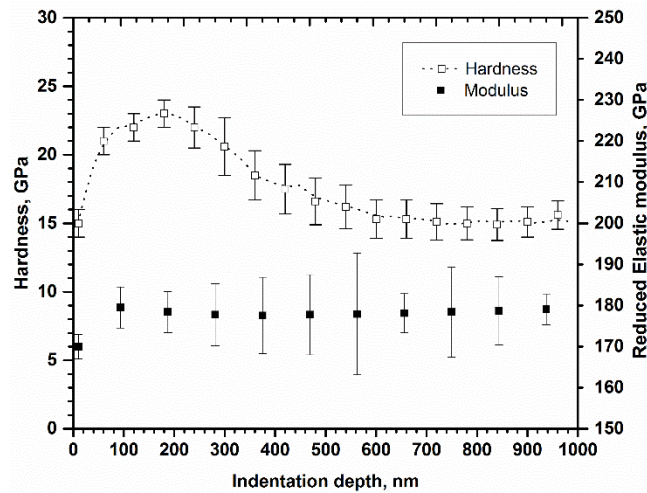

Figure 5. Nanohardness and reduced elastic modulus of the carbon film measured as a function of the indentation depth.

The maximum nanohardness of treated samples increases by 200% than that of the bare substrate (see table 1), i.e. a nanohardness of ~ 23 GPa is reached at ~180 nm depth, which is consistent with the general observance of sustaining depth < 10% of the coating thickness (2.8 µm) to minimise substrate effects. The behaviour of the indentation depth less than 180 nm could be attributed to the surface imperfections such as roughness. However, as the depth increases ($\geq$ 10% of the coating thickness), the nanohardness reduces, indicating that the substrate is strongly influencing the hardness behaviour [31], namely, nanohardness of the coating was dependent on the indentation depth. On the contrary, the reduced elastic modulus has little difference between bare substrate and the treated steel, namely, the reduced elastic modulus is approximately independent of the indentation depths. It is noticeable from Fig. 5 that variations in the surface topography led to the scatter in measured values from 200 nm inwards. Clearly, the influence of the softer steel substrate becomes more prominent when indentation depth overflows that 10 % of the coating thickness. The hardness and elastic modulus of the H-DLC coating is 20^{+3}_{-0} GPa and 180 ± 10 GPa, respectively.

Although hardness is a material property usually considered as crucial to define wear resistance, the elastic modulus also protrudes on wear behaviour, specifically, the elastic strain to failure, which, according to Leyland and Mathews [32], is related to the ratio of hardness (H) and elastic modulus (E). Thus, the H/E ratio is hypothesised to be an indication of the wear rate of the film, described as the deformation relative to yielding. Values of H and $E^* \rightarrow E^* = E / (1 - v^2)$ allow simple calculation of the ratio H^3/E^{*2}, which gives information on the resistance to plastic deformation. The higher the ratio is, the higher the resistance of the coating to plastic deformation. Therefore, taking H = 20 GPa and E=208 GPa (determined from $E_{reduced\ DLC}$ = 179 GPa, v_{DLC} = 0.3, $E_{indenter}$ = 1140, $v_{indenter}$ =0.07) gives H^3/E^{*2} = 0.1. Similar values for W-DLC coatings have been reported in other studies [20]. Wear index for Si-DLC and DLC coatings have been reported as 0.15 and 0.12 respectively.

Raman spectroscopy is the selective technique to acquire information regarding the bonding structure of hydrogenated carbon films. Fig. 6 shows the Raman spectra performed in air at 40% RH of the H-DLC coating as deposited on steel plate. The spectra was deconvoluted using Gaussian and Lorentzian functions, where first, a linear background was subtracted. In the plot, two distribution bands in the 900-1800 cm^{-1} range are shown. These two bands are well defined, as the disorder (D) and graphite (G) ones that initiate from sp^2 sites, due to the fact that the 488 nm excitation resonates with $\pi - \pi^*$ transitions at sp^2 sites, and in this case the band D dominates over the contribution of sp^3 sites [33]. The G band (graphitic) is centred at 1545 cm^{-1} for visible excitation. The D band (shouldered) at 1363 cm^{-1} is attributed to bond angle disorder in the graphite-like micro domains affected by sp^3 bond. Indeed, this band represents the breathing modes of sp^2 atoms in aromatic clusters in hydrogenated carbon films [34]. The broadening of the lines confirms the amorphous hydrocarbon molecules of this coating, in particular, due to the fact that there are no bands and peaks at wave numbers below 800 cm^{-1}. The integrated intensity ratio of the Gaussian line shape analysis for the above spectrum was I_D/I_G = 0.49 and the FWHM (cm^{-1}) for D and G peaks were 347 and 168 respectively.
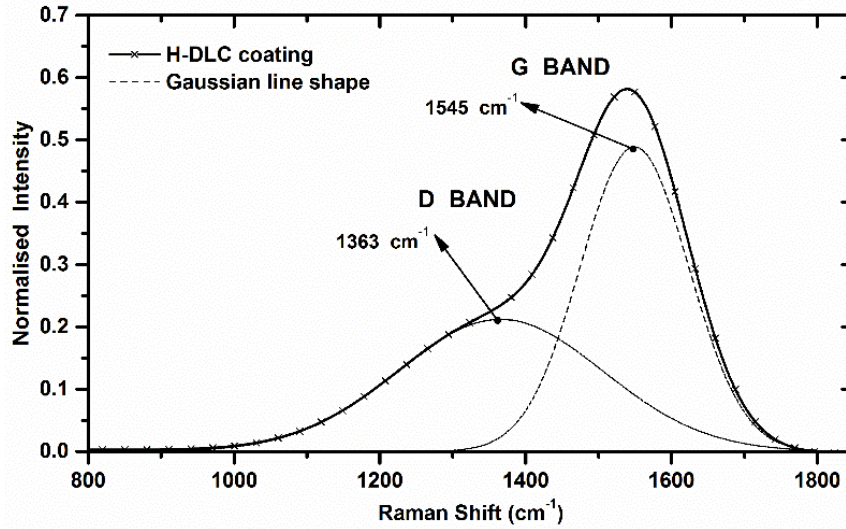
Figure 6. Raman spectra of the H-DLC before the friction test.

3.2 Tribological behaviour

The variation of the coefficient of friction (μ) as a function of sliding distance in dry conditions and under several applied normal loads is displayed in Fig. 7. At the beginning of the test in dry condition, the CoF for 10 and 20 N loads increased progressively with the increasing of the sliding distance until it reached an average upper value of 0.22-0.23, respectively, and then, a slightly decreasing trend is visible until it levelled off with average values of 0.20-0.21. This initial rise in the CoF is attributed to the initial high roughness (Fig. 8a) and reduced contact area between the interfaces. Due to sliding, the rough surface features smoothen as a result of the elastic and plastic effects of the frictional forces acting on the coating, which in turn increase the contact area that is strongly associated to the CoF, specifically its appearance and surface hardness corresponding to the deformation resistance of the contact area (recalling the well-known relationship $\tau = \dfrac{F\mu}{A} \Rightarrow H = \dfrac{F}{A}$, where A would be the real contact area, τ the shear strength of the junction, F the applied normal load, and H the mean pressure on an asperity or simply the local hardness of the material). As the sliding continues, the slightly decreasing trend of the CoF is linked, on one hand, to the low magnitude of the applied normal load, which produces a certain amount of friction-induced localized heating and melting of the contact asperities, which may slowly but progressively generate an amorphized transfer layer capable of contributing in the reduction of the CoF [35]. The surface roughness of selected specimen at the end of

13

the sliding is shown in Fig. 8b. On the other hand, the elimination of free σ-bonds on sliding surfaces also determines the levels of reduction in friction. Here, atomic and/or molecular hydrogen within the coating (interstitially accommodated within the H-DLC structure), continuously replenishes and terminates the σ-bonds that were inherently exposed by the dynamic contact [36]. In contrast, the corresponding frictional features for higher loads, namely, 30-50 N loads exhibited a decreasing trend of the CoF from the running-in stage. In this regard, the contact pressure is higher and temperature between the pin and the coating goes up because of the higher pushing forces, and thus, roughness asperities plastically deform with bending and drawing movements; and as a result, there appears to be a rapid development of a graphite-like lubricious tribolayer. In addition, when higher loads are applied on the coating surface, it has been reported that self-alignment of graphitized/amorphized tribolayer and effective passivation of dangling bonds by scattered hydrogen atoms and/or molecules in ambient atmosphere contribute in the lessening the CoF [11, 36, 37]. In Fig. 8c, the worn surface at the end of the sliding is shown. Regardless of the initial tribological discrepancies, it is very distinguishable in Fig. 7 that steady-state levels of friction commence in the range of 1740-1800 m of rubbing for all loads.
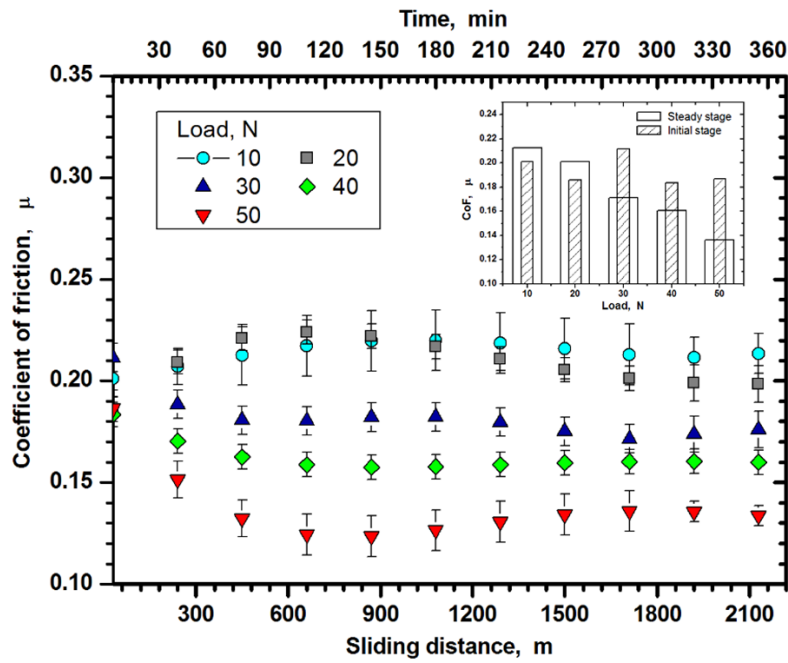
Figure 7. Evolution of the frictional behaviour of the reciprocating pin-on-plate of H-DLC coated steel subjected to different loads and at 0.1 m s^{-1}. The inset graph shows the average CoF values for both the initial and the steady-stages versus applied loads.

The maximum average value of the steady-state coefficient of friction was 0.21, under a normal load of 10 N and a minimum average value of 0.13 was obtained for a normal load of 50 N. These levels of CoF resemble to those put forward in [38], under similar preparation and test conditions. In comparison, other studies under similar conditions [26, 39] showed steady-state values that ranged from 0.25 to 0.6, which are higher than those in the actual study. Furthermore, in [40] a H-DLC coating with an adhesion layer of Cr was deposited on a particular rubber via unbalanced magnetron reactive sputtering from a WC target in a C_2H_2/Ar plasma, and tested under dry sliding condition against an AISI 52100 ball. Its tribological performance in terms of CoF spanned between 0.2 - 0.25, which is comparable to the values of CoF for the lower loads in this work. On the whole, the coatings could withstand film failure or delamination and the coefficient of friction displayed a dependence on the applied force for the steady stage as can be noticed in the inset graph of the Fig. 7.
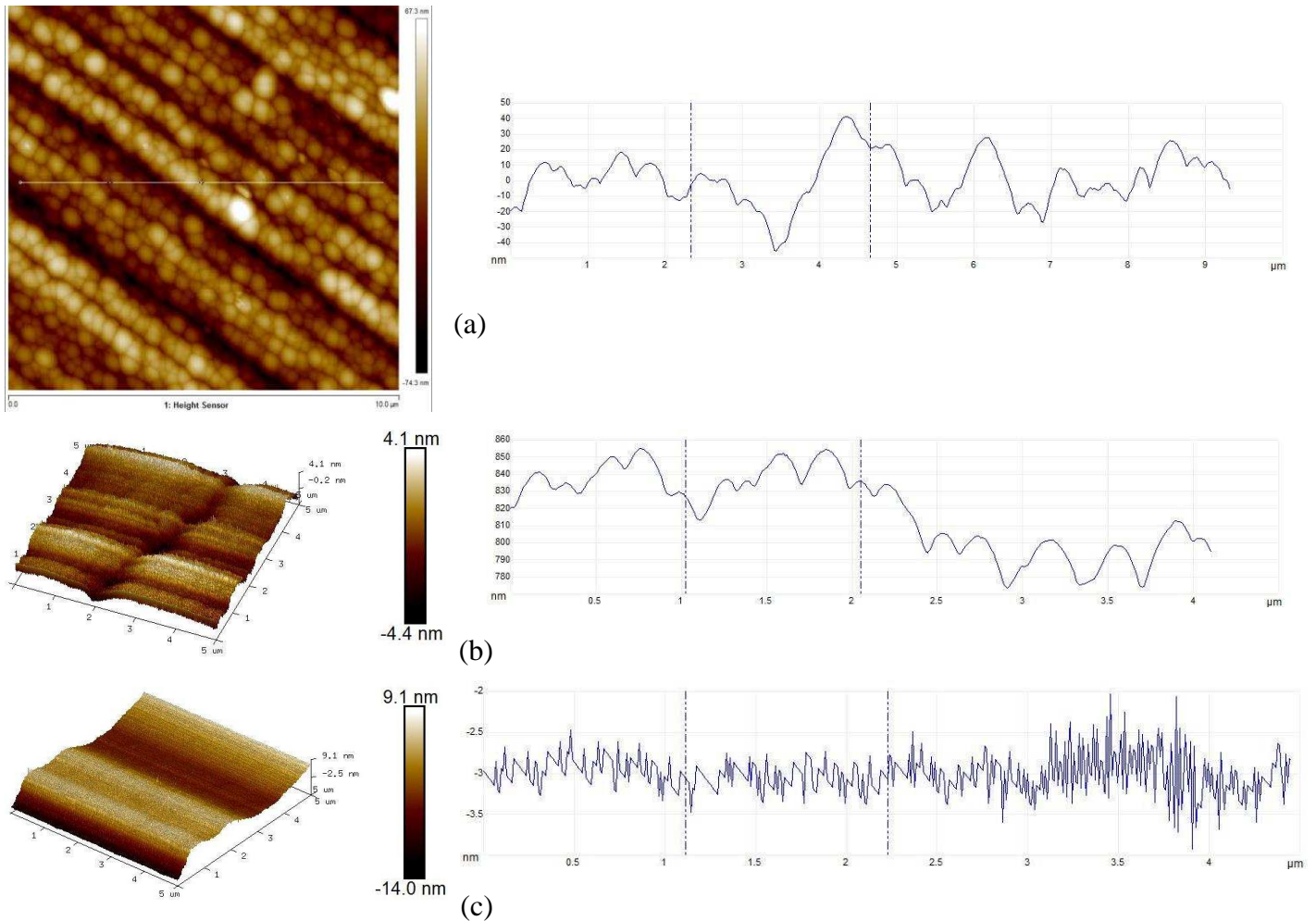
Figure 8. AFM images of the H-DCL coatings and their averaged surface roughness for (a) as deposited, (b) selected worn area of 5µm x 5µm under a 20 N applied load, and (c) selected worn area after sliding with a 50 N applied load.

The wear scars of the contacts H-DLC/steel inscribed in dry condition are significantly shallow for each of the applied normal loads, as confirmed by the surface profile scanning of the wear scars which can be seen in the representative scars depicted in Fig. 9. On this context, the maximum levels of wear depth along the transverse section of the sliding direction of wear scars, i.e. the Y profiles in Fig. 9 (c and f), did not exceed 1.5 µm. This latter observation shows that the penetration depth is lower than the coating thickness. It is also noticeable from the three dimensional pictures of the plate scars shown in Figs. 9 (a and d), that despite of the apparent removal of material as a result of the tangential forces acting directly on the surface of the coating, there is no sign of sharp interfacial brittle crack generation.

It can be established that the coating deforms plastically and bends into the coating-remains and also transfers to the counterbody as will be shown later in this section. These finding agree with the scratch results, i.e. there is plastic deformation observed at the formed groove by the continuous increase of the load up to a critical load greater than 80 N without brittle crack or interfacial spallation. It seems to be apparent, that ductility of the duplex-layered coating allowed for an effective relaxation of the residual stresses (< 1 GPa as mentioned in section 2.1) provoked by the chromium layer, which indeed minimized the crack induced surface and interfacial fracture.
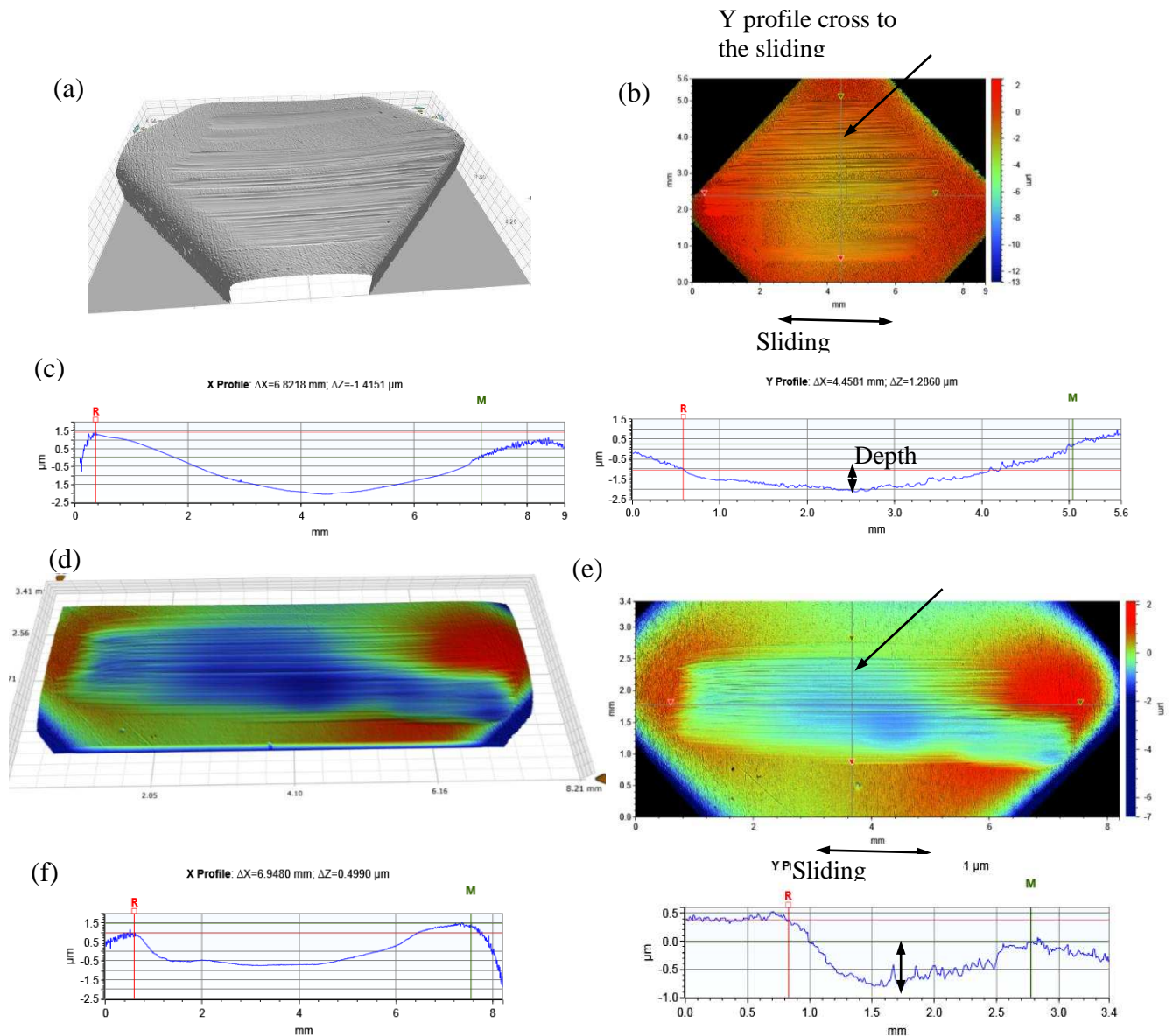

Figure 9. Representative wear scars on the WC/H-DLC coated plates after 2160 m sliding distance, showing the wear depths both parallel and transverse to the sliding direction for (a-c) 10 N and (d-f) 50 N.

In Fig. 10, the specific wear rates of the H-DLC coatings are depicted. Under the same sliding velocity condition (0.1 m/s), with the increase in normal load, the average specific wear rates decrease. The maximum and minimum specific wear rates are 14×10^{-8} and 5.5×10^{-8} mm^{-3}/N m, respectively. The former under a normal load of 10 N and the latter under a normal load of 50 N for 6 h or 2160 m dry sliding. The reduction in specific wear rate seems to be abetted by the formation of a transfer layer on the counter-layer, because of structural transformations triggered by the normal load applied during the sliding. Among these structural effects, the re-crystallisation process becomes very active at the contact interface in such a way that, due to the reciprocating sliding, a re-orientation of the re-crystallised layers brings the basal planes parallel to the top surface of the coating with the consequent reduction in the wearing rate [41]. Specifically, the sliding-induced localised annealing at the contact asperities, likely causes a gradual destabilization of the carbon-hydrogen bond in the sp^3 tetrahedral structure and as a result, a transformation of this sp^3 structure into a graphite-like sp^2 structure takes place [11]. These changes in the chemical behaviour of the near-surface structure of the worn coatings were characterized by Raman spectroscopy and are shown in Fig. 11. The spectrum taken from the wear tracks of the high frequency peaks (G) have shifted to a higher frequency nearing the graphite frequency. Particularly, if it is considered that hydrogenated DLC Raman spectra are commonly composed of the high and low frequency peaks oscillating at 1540 cm^{-1} for the graphite-like sp^2-bonded carbon and 1360 cm^{-1} for the sp^3-bonded phase [9]. There is also an increase in the intensity of the low frequency peak due to D band graphite contributions, since the I_D/I_G ratio is also proportional to sp^2/sp^3 ratio. Therefore, the wear track H-DLC surface undergoes certain amount of changes in the chemical behaviour due to the strain-stress state of the sliding surfaces and the chemical reactions with ambient atmospheric contamination, leading to graphitization/amorphization to some extent.
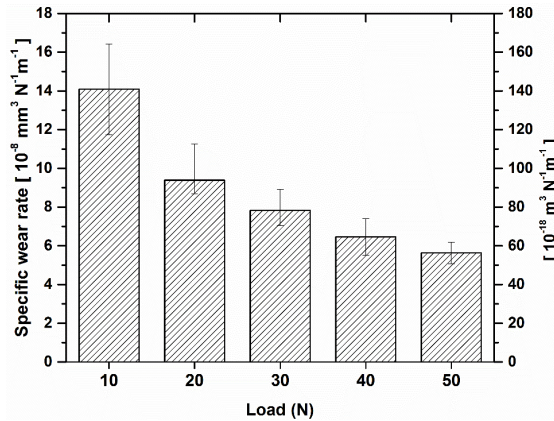
Figure 10. Dimensional wear coefficients of the WC/H-DLC assessed at several loads. Error bars are the standard deviation from the average values of three weight measurements.

In addition, because of atmospheric contamination, it is well-known that effective passivation takes place, i.e. the internal hydrogen atoms in the coating strongly interact with the external micro molecules of water present in the humid environment, provoking a strong adhesion mainly caused by the capillary force induced union. This should result in a high wear rate due to the elevated adhesion, but as observed in Fig. 10, there is a clear reduction in the wear rate as the load rises just like it occurred for the CoF (Fig. 7). As expected, under dry conditions, the aforementioned graphite-like sp^2 structure contributed to the transfer of C from H-DLC to the steel pin with a consequent reduction in the adhesion and friction due to the fact that the contact was carbon-on-carbon rather than carbon-on-steel. This was verified, firstly, by measuring the wear depth of the H-DLC coating at the end of the sliding tests. The coating presented DLC after the rubbing and also there was no transferred material from the steel pin to the coated plate as can be observed in Fig. 12. The top of the a-C:H was partially worn holding approximately 0.6 µm thickness with carbon and tungsten to a lesser extent. The Cr interlayer remained intact for all applied loads. And secondly, Raman analyses were carried out on the wear surfaces of the plates (Fig. 11), these appeared to have a tendency to a graphitic character, which clearly indicates the carbon nature of the tribolayer formation at the contact.
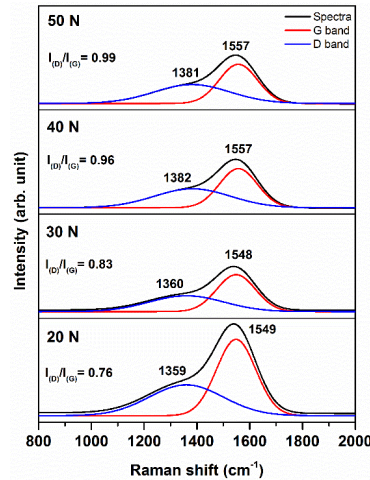
Figure 11. Raman spectroscopy taken from wear track zones of the coated plate after testing, and for different applied loads.
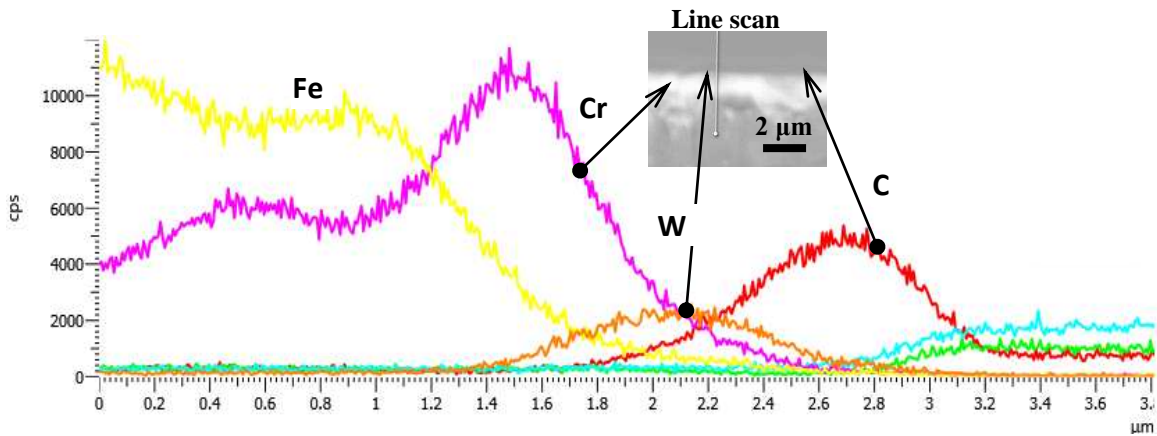

Figure 12. Representative chemical composition profile taken on a worn region of the H-DLC coating after the sliding test for a 40 N applied load.

Secondly, by analysing the transfer layer on the wear scars on the AISI 52100 steel pins. Raman spectroscopy was utilised to identify the tribolayer formations on these counterparts. The spectra were measured on the several zones of the wear scars and a representative spectrum of two different loads is shown in Fig. 13. Evidently the signals are dissimilar to those taken on the wear tracks of the coated plates (Fig. 11). This is because the quantities of transferred carbon to the steel pin are much lower than those present in the deposited bulk carbon film on the steel plate, and therefore, the thickness of

transferred material appears to be non-homogeneous as can be seen in the inset picture of the wear scar on the steel pin in Fig. 13. In the same inset image, it is observed that dark-grey transfer layers are present on the wear scar and along the sliding direction in the shape of long stripes. It also can be corroborated from the signals depicted in the same Fig. 13, as the intensities were very much lower than those for the plate worn tracks, which suggests that the amount of graphite formed was rather limited. In addition, the Raman spectra of the transferred layer exhibited two broad and strong peaks with wave numbers oscillating at 1589-1609 cm^{-1} and 1328-1358 cm^{-1}. These peaks are close to the G and D band peaks of the natural graphite and their shapes resembles that of highly disordered graphite [15]. Therefore, the surface of the coating wear track and the tribolayer formations on the pin wear scars appeared to have a graphitic character, confirming the carbon-carbon contact.
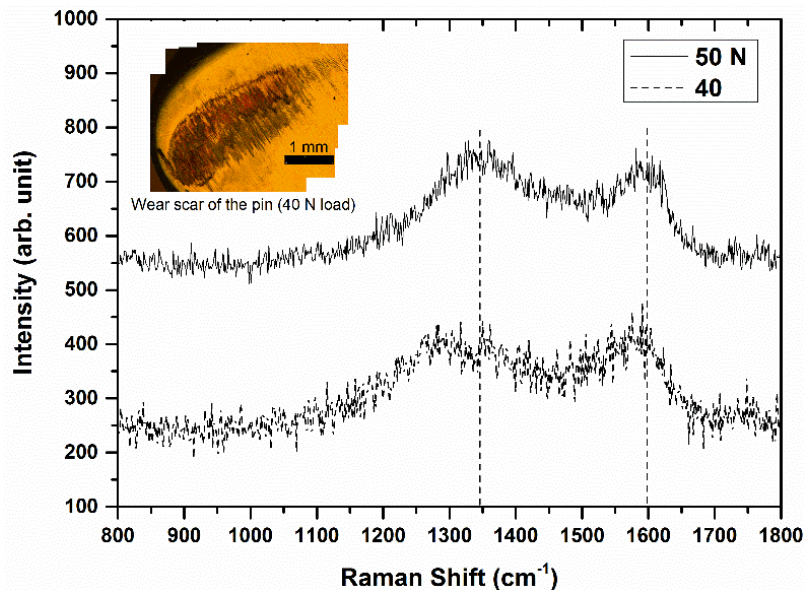

Figure 13. Selected Raman spectra of the steel pins wear scars after sliding against H-DLC coating. Tribotest conditions were: 2300 m sliding distance in humid air (45 ± 5 % RH) and sliding velocity of 0.1 m s^{-1}. The inset image shows the wear scar on the steel pin for a 40 N applied load.

3.3 Phase transition analysis

There is a strong indication of DLC coating graphitisation from prior observations as well as from the correlations between friction and wear behaviours. Under dry sliding conditions, temperature and high contact stresses appear to be central in the breakdown of the hydrogenated DLC coating [30]. The rationale comes out of the pressure induced temperature at the sliding contact; the hydrogen atoms are

unbound from the diamond-like matrix and as a result, feebly hydrogen-depleted sites turn out. This weak surface is then deformed by the high contact stresses turning into a graphitic structure (from sp^3 bonded carbon to sp^2 bonded carbon) which favours a reduction of friction [42]. The carbon transition temperature for hydrogen desorption mostly depends on the initial hydrogen content and the sliding contact pressure. As a qualitative account on the transition observed in this study, the Clapeyron law [43] can be used for the present discussion. It states that, the increase of Hertzian contact pressure leads to a decrease in the graphitisation temperature as long as the specific volume of hydrogenated coatings is higher than the dehydrogenated coatings, which can be mathematically expressed by the following relationship:

$$\frac{dP}{dT} = \frac{L}{T(v_f - v_i)} \tag{3}$$

Note that $v_i > v_f$ because if the density of a hydrogenated film decreases when the hydrogen content increases, then $dP/dT < 0$.

Where L is the transition phase energy of diamond (15.6×10^4 J/kg) [43], v_i is the hydrogenated film specific volume (from $v_i = 0.294 \times 10^{-3}$ to 0.416×10^{-3} m^3/kg, depending on the amount of hydrogen incorporated in the film), v_f is the dehydrogenated film specific volume ($v_f = 0.284 \times 10^{-3}$ m^3/kg) [44] and T is the transition temperature of coating in vacuum (around 400 °C [45]). The solution of the differential equation (3) is given by the following equation:

$$T = T_c \exp\left(\frac{v_f - v_i}{L} \Delta P\right) \text{ with } \Delta P = P_{max} - P_a \tag{4}$$

Where P_{max} is the Hertzian contact pressure given by $P_{max} = \frac{1}{\pi}\left(\frac{6FE^2}{R^2}\right)^{\frac{1}{3}}$ and P_a is the atmospheric pressure (0.1 MPa). F is the applied load, R is the radius of the pin (R = 110 mm) and

$E = \left(\frac{1-v_1^2}{E_1} + \frac{1-v_2^2}{E_2}\right)^{-1}$. E_1 = Elastic moduli of the steel pin (~160 GPa), E_2 = Elastic moduli of the H-DLC (180 GPa), v_1 = Poisson ratio of the steel pin (0.3) and v_2 = Poisson ratio of the coating (0.28).

When all the above parameters for the present study are used in Eq. (4), it can be shown that the phase transition temperature of the H-DLC coating decreases with an increase of contact stress but also decreases abruptly with an increase of hydrogenated coating specific volume, as illustrated in Fig. 14. Specifically, if it is taken into account that the mass density of H-DLC oscillates from 1.9-3.0 g/cm^3

22

[46], it can then be considered a density of 2.5 g/cm^3 (0.4 x 10^{-3} m^3/kg) for the actual coating. In the process, the transition temperature can be decreased to 300 - 325 °C, for contact stresses ranging from 0.1 - 0.2 GPa, i.e., when the applied normal loads vary between 10 and 50 N.
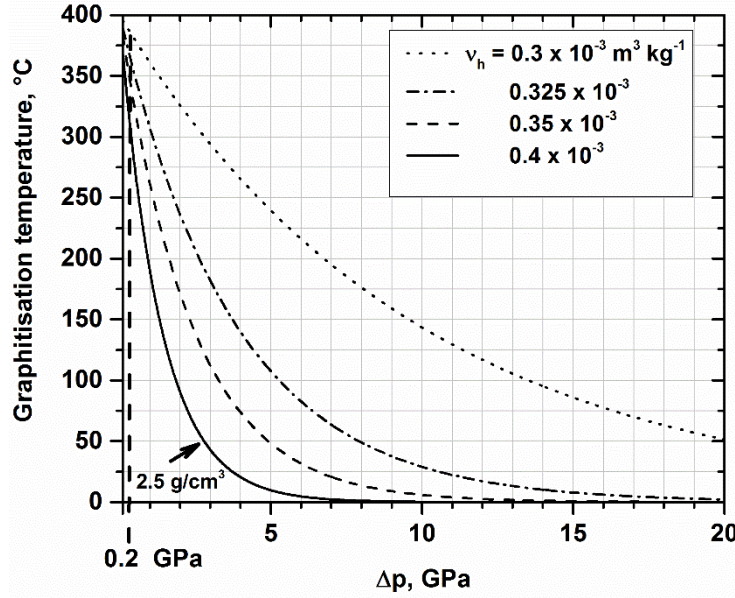

Figure 14. Graphitisation temperature of the H-DLC coating as a function of specific volume of hydrogenated coating and contact pressure. Plots are obtained from Eq. (4).

In order to determine if the surface temperature of the two sliding bodies in contact is sufficiently high as to reach the graphitisation temperature, the following flash temperature relationship [11] can be used to estimate an approximate of the induced temperature rise due to the frictional heat at the contact area.

$$\Delta T = \mu Pv / 4J(K_1 + K_2)a \quad \text{with } a = \left(\frac{P}{\pi H}\right)^{\frac{1}{2}} \tag{5}$$

where μ is the coefficient of friction, P is the applied load, v is the sliding velocity, K_1 and K_2, are the thermal conductivities of the coating and the steel pin, J is the Joule´s constant (J = 1), a is the contact radius of the real contact area, and H is the measured hardness of the H-DLC coating. Using Eq. (5) and the actual experimental data, the calculated surface temperature rise when the applied load varies are enumerated in Table 3.

23

Table 3.   Estimated flash temperature.

Constants		P (N)	a (µm)	μ^b	ΔT
[a]K_1 (W/mK) Steel	17[a]	10	11.8	0.21	221
[a]K_2 (W/mK) H-DLC	3[a]	20	16.6	0.21	315.6
H (GPa)	23	30	20.4	0.19	349.7
v (m/s)	0.1	40	23.5	0.17	361.3
		50	26.3	0.15	356.4

[a]Ref. [47], [b]μ ~ initial at 240 m sliding distance.

The calculated flash temperatures eased the graphitisation process for the applied loads of 30 - 50 N, due to the fact that exceeded the phase transition temperatures (~325 °C). This result appears to agree with the frictional behaviour shown in Fig. 7, since for such loads the very initial values of CoF exhibited a slowly decrease to almost constant value during the following sliding distance, which could be an indication of an early graphitisation degree of the H-DLC surface layer. In the case of the loads 10 and 20 N, the calculated temperature rise at contact asperities was lower than the calculated graphitisation temperature. These results also seemed to agree with the frictional tendencies for such loads, since the CoF slowly increase to a maximum and eventually decrease to almost constant value (Fig. 7). The estimated flash temperature is high enough to change the state of the contact interfases in the way of desorbed hydrogen. Therefore, the edge sites multiply themselves and there is an increase in the adhesion of the tribopair. This may explain that increasing values of CoF. As the sliding continue and since there is hydrogen on the friction track, hydrogen desorption from the surface is also progressive generating inactive sites and in consequence CoF reduces. The extremely unstable carbon atoms from the active sites may attempt to form more stable structures, but because of the contact stress, the active surface can be dislocated facilitating the transformation of the sp^2 structure on the surface of the coating. In addition, it has been analysed in previous research [48] that the presence of wear debris in the tribopair´s interface can promote the graphitisation of amorphous hydrocarbon molecules, by virtue of a rise in the Hertzian contact pressure at surface asperities, which brings down the transition temperature.

4.   Conclusions

A hydrogenated Diamond-like Carbon has been characterised both prior to, and following tribological testing. Friction and wear behaviour under dry unlubricated conditions of a [WC/a-C:H]/steel contact has been assessed for different normal loads in ambient atmosphere. The adhesive strength of the

coating was found to be more than acceptable for industrial applications with a scratch resistance above 80 N. At the levelled off stage, coefficients of friction decrease with the increase of the applied normal load. This is because, depending on this increase in the normal load, the chemical composition of the coating can be seen to alter in the form of a graphitized wear surface and a degree of transfer layer formation also takes place, as revealed by the Raman analyses. The maximum and minimum values of average coefficient of friction after 2160 m rubbing were, 0.21 under 100 MPa maximum contact pressure at 0.1 m/s, and 0.13 under 190 MPa maximum contact pressure at the same velocity. Specific wear rate of the H-DLC/steel tribocouple behaves as the degree of graphitisation does, which, in turn, is governed by the severity of the applied load. So, in this study, the specific wear rate decreased with the increase in normal load. The formation of a protective transferred layer on the counterpart made carbon-carbon contact conditions with a consequent reduction in wear of both mating surfaces. The maximum wear rate value for the H-DLC coatings was 14×10^{-8} mm^{-3} /N m under a normal load of 10 N and 5.5×10^{-8} mm^{-3} /N m under a normal load of 50 N, following 2160 m of dry sliding. According to the outcomes from the present research, the H-DLC coating could be useful for wide range of industrial applications such as automotive, aircraft and machine components.

Acknowledgement

References

[1] D. Roth, B. Rau, S. Roth, J. Mai, K.H. Dittrich, Large area and three-dimensional deposition of diamond-like carbon films for industrial applications, Surf. Coat. Technol. 74–75, Part 2 (1995) 637-641.

[2] A. Grill, Diamond-like carbon: state of the art, Diam. Relat. Mater. 8 (1999) 428-434.

[3] A. Matthews, S.S. Eskildsen, Engineering applications for diamond-like carbon, Diam. Relat. Mater. 3 (1994) 902-911.

[4] J. Robertson, Comparison of diamond-like carbon to diamond for applications, Phys, Status Solidi A 205 (2008) 2233-2244.

[5] W. Tillmann, F. Hoffmann, S. Momeni, R. Heller, Hydrogen quantification of magnetron sputtered hydrogenated amorphous carbon (a-C:H) coatings produced at various bias voltages and their tribological behavior under different humidity levels, Surf. Coat. Technol. 206 (2011) 1705-1710.

[6] L. Cui, Z. Lu, L. Wang, Probing the low-friction mechanism of diamond-like carbon by varying of sliding velocity and vacuum pressure, Carbon 66 (2014) 259-266.

[7] J.C. Sánchez-López, A. Erdemir, C. Donnet, T.C. Rojas, Friction-induced structural transformations of diamondlike carbon coatings under various atmospheres, Surf. Coat. Technol. 163–164 (2003) 444-450.

[8] J. Stallard, D. Mercs, M. Jarratt, D.G. Teer, P.H. Shipway, A study of the tribological behaviour of three carbon-based coatings, tested in air, water and oil environments at high loads, Surf. Coat. Technol. 177–178 (2004) 545-551.

[9] A.A. Voevodin, S.D. Walck, J.S. Zabinski, Architecture of multilayer nanocomposite coatings with super-hard diamond-like carbon layers for wear protection at high contact loads, Wear 203–204 (1997) 516-527.

[10] N. Sharma, N. Kumar, S. Dash, C.R. Das, R.V. Subba Rao, A.K. Tyagi, B. Raj, Scratch resistance and tribological properties of DLC coatings under dry and lubrication conditions, Tribol. Int. 56 (2012) 129-140.

[11] Y. Liu, A. Erdemir, E.I. Meletis, A study of the wear mechanism of diamond-like carbon films, Surf. Coat. Technol. 82 (1996) 48-56.

[12] S.Y. Luo, J.K. Kuo, T.J. Tsai, C.W. Dai, A study of the wear behavior of diamond-like carbon films under the dry reciprocating sliding contact, Wear 249 (2001) 800-807.

[13] H. Ronkainen, J. Koskinen, J. Likonen, S. Varjus, J. Vihersalo, Characterization of wear surfaces in dry sliding of steel and alumina on hydrogenated and hydrogen-free carbon films, Diam. Relat. Mater. 3 (1994) 1329-1336.

[14] J.L. Mo, M.H. Zhu, Tribological investigation of WC/C coating under dry sliding conditions, Wear 271 (2011) 1998-2005.

[15] D. Sheeja, B.K. Tay, S.P. Lau, X. Shi, Tribological properties and adhesive strength of DLC coatings prepared under different substrate bias voltages, Wear 249 (2001) 433-439.

[16] Y. Wang, Y. Ye, H. Li, L. Ji, Y. Wang, X. Liu, J. Chen, H. Zhou, Microstructure and tribological properties of the a-C:H films deposited by magnetron sputtering with CH4/Ar mixture, Surf. Coat. Technol. 205 (2011) 4577-4581.

[17] E.-S. Yoon, H. Kong, K.-R. Lee, Tribological behavior of sliding diamond-like carbon films under various environments, Wear 217 (1998) 262-270.

[18] K.J. Clay, S.P. Speakman, N.A. Morrison, N. Tomozeiu, W.I. Milne, A. Kapoor, Material properties and tribological performance of rf-PECVD deposited DLC coatings, Diam. Relat. Mater. 7 (1998) 1100-1107.

[19] M. Keunecke, K. Weigel, K. Bewilogua, R. Cremer, H.G. Fuss, Preparation and comparison of a-C:H coatings using reactive sputter techniques, Thin Solid Films 518 (2009) 1465-1469.

[20] L.B. Austin, Evaluation and optimisation of diamond-like carbon for tribological applications, in: School of Mechanical Engineering, The University of Leeds, Leeds, U.K., 2014.

[21] M. Kalin, M. Polajnar, The correlation between the surface energy, the contact angle and the spreading parameter, and their relevance for the wetting behaviour of DLC with lubricating oils, Tribol. Int. 66 (2013) 225-233.

[22] A. Neville, A. Morina, T. Haque, M. Voong, Compatibility between tribological surfaces and lubricant additives—How friction and wear reduction can be controlled by surface/lube synergies, Tribol. Int. 40 (2007) 1680-1695.

[23] A. Morina, H. Zhao, J.F.W. Mosselmans, In-situ reflection-XANES study of ZDDP and MoDTC lubricant films formed on steel and diamond like carbon (DLC) surfaces, Appl. Surf. Sci. 297 (2014) 167-175.

[24] M.I. de Barros'Bouchet, J.M. Martin, T. Le-Mogne, B. Vacher, Boundary lubrication mechanisms of carbon coatings by MoDTC and ZDDP additives, Tribol. Int. 38 (2005) 257-264.

[25] C. Strondl, N.M. Carvalho, J.T.M. De Hosson, T.G. Krug, Influence of energetic ion bombardment on W-C:H coatings deposited with W and WC targets, Surf. Coat. Technol. 200 (2005) 1142-1146.

[26] O. Wänstrand, M. Larsson, P. Hedenqvist, Mechanical and tribological evaluation of PVD WC/C coatings, Surf. Coat. Technol. 111 (1999) 247-254.

[27] G.G. Stoney, The Tension of Metallic Films Deposited by Electrolysis, Proceedings of the Royal Society London A 82 (1909) 172-175.

[28] M.A. Hopcroft, What is the Young's Modulus of Silicon?, Journal of Microelectromechanical systems (IEEE)

 9 (2010) 229-238.

[29] S. Johansson, P.H. Nilsson, R. Ohlsson, B.-G. Rosén, Experimental friction evaluation of cylinder liner/piston ring contact, Wear 271 (2011) 625-633.

[30] C.W. Ong, X.A. Zhao, J.T. Cheung, S.K. Lam, Y. Liu, C.L. Choy, P.W. Chan, Thermal stability of pulsed laser deposited diamond-like carbon films, Thin Solid Films 258 (1995) 34-39.

[31] T.H. Zhang, Y. Huan, Nanoindentation and nanoscratch behaviors of DLC coatings on different steel substrates, Compos. Sci. Tech. 65 (2005) 1409-1413.

[32] A. Leyland, A. Matthews, On the significance of the H/E ratio in wear control: a nanocomposite coating approach to optimised tribological behaviour, Wear 246 (2000) 1-11.

[33] J. Robertson, Diamond-like amorphous carbon, Mat. Sci. Eng. R 37 (2002) 129-281.

[34] A.C. Ferrari, J. Robertson, Interpretation of Raman spectra of disordered and amorphous carbon, Phys. Rev. B 61 (2000) 14095-14107.

[35] Y. Liu, A. Erdemir, E.I. Meletis, An investigation of the relationship between graphitization and frictional behavior of DLC coatings, Surf. Coat. Technol. 86–87, Part 2 (1996) 564-568.

[36] A. Erdemir, The role of hydrogen in tribological properties of diamond-like carbon films, Surf. Coat. Technol. 146–147 (2001) 292-297.

[37] J.F. Lin, P.J. Wei, J.C. Pan, C.-F. Ai, Effect of nitrogen content at coating film and film thickness on nanohardness and Young's modulus of hydrogenated carbon films, Diam. Relat. Mater. 13 (2004) 42-53.

[38] D.-W. Kim, K.-W. Kim, Effects of sliding velocity and normal load on friction and wear characteristics of multi-layered diamond-like carbon (DLC) coating prepared by reactive sputtering, Wear 297 (2013) 722-730.

[39] B. Vengudusamy, A. Grafl, K. Preinfalk, Tribological properties of hydrogenated amorphous carbon under dry and lubricated conditions, Diam. Relat. Mater. 41 (2014) 53-64.

[40] Y.T. Pei, X.L. Bui, X.B. Zhou, J.T.M. De Hosson, Tribological behavior of W-DLC coated rubber seals, Surf. Coat. Technol. 202 (2008) 1869-1875.

[41] S. Yang, X. Li, N.M. Renevier, D.G. Teer, Tribological properties and wear mechanism of sputtered C/Cr coating, Surf. Coat. Technol. 142–144 (2001) 85-93.

[42] D.R. Tallant, J.E. Parmeter, M.P. Siegal, R.L. Simpson, The thermal stability of diamond-like carbon, Diam. Relat. Mater. 4 (1995) 191-199.

[43] T. Le Huu, H. Zaidi, D. Paulmier, P. Voumard, Transformation of sp3 to sp2 sites of diamond like carbon coatings during friction in vacuum and under water vapour environment, Thin Solid Films 290–291 (1996) 126-130.

[44] A.H. Deutchman, R.J. Partyka, Diamond Film Deposition, Adv. Mater. Process. 6 (1989) 29-33.

[45] W. Piekarczyk, Diamond-vapour interface and processes proceeding on it during growth of diamond crystals I. Diamond (111) face, J. Cryst. Growth 119 (1992) 345-362.

[46] C. Donnet, A. Grill, Friction control of diamond-like carbon coatings, Surf. Coat. Technol. 94–95 (1997) 456-462.

[47] Z.F. Zhou, K.Y. Li, I. Bello, C.S. Lee, S.T. Lee, Study of tribological performance of ECR–CVD diamond-like carbon coatings on steel substrates: Part 2. The analysis of wear mechanism, Wear 258 (2005) 1589-1599.

[48] T. Haque, A. Morina, A. Neville, R. Kapadia, S. Arrowsmith, Effect of oil additives on the durability of hydrogenated DLC coating under boundary lubrication conditions, Wear 266 (2009) 147-157.

FIGURE CAPTIONS

Figure 1. AFM image of the bare H-DLC coating.

Figure 2. Overview of the reciprocating pin-on-plate set up.

Figure 3. (a) SEM micrograph in cross section and (b) the composition profile of the DLC coating deposited on AISI 53100 steel. The elements Cl and Ag are contaminants due to the manipulation of the sample for the analysis.

Figure 4. Scratch induced acoustic emission test on the H-DLC deposited by MW-PECVD.

Figure 5. Nanohardness and reduced elastic modulus of the carbon film measured as a function of the indentation depth.

Figure 6. Raman spectra of the H-DLC before the friction test.

Figure 7. Evolution of the frictional behaviour of the reciprocating pin-on-plate of H-DLC coated steel subjected to different loads and at 0.1 m s^{-1}. The inset graph shows the average CoF values for both the initial and the steady-stages versus applied loads.

Figure 8. AFM images of the H-DCL coatings and their averaged surface roughness for (a) as deposited, (b) selected worn area of 5µm x 5µm under a 20 N applied load, and (c) selected worn area after sliding with a 50 N applied load.

Figure 9. Representative wear scars on the WC/H-DLC coated plates after 2160 m sliding distance, showing the wear depths both parallel and transverse to the sliding direction for (a-c) 10 N and (d-f) 50 N.

Figure 10. Dimensional wear coefficients of the WC/H-DLC assessed at several loads. Error bars are the standard deviation from the average values of three weight measurements.

Figure 11. Raman spectroscopy taken from wear track zones of the coated plate after testing, and for different applied loads.

Figure 12. Representative chemical composition profile taken on a worn region of the H-DLC coating after the sliding test for a 40 N applied load.

Figure 13. Selected Raman spectra of the steel pins wear scars after sliding against H-DLC coating. Tribotest conditions were: 2300 m sliding distance in humid air (45 ± 5 % RH) and sliding velocity of 0.1 m s^{-1}. The inset image shows the wear scar on the steel pin for a 40 N applied load.

Figure 14. Graphitisation temperature of the H-DLC coating as a function of specific volume of hydrogenated coating and contact pressure. Plots are obtained from Eq. (4).